IEICE TRANSACTIONS

on Electronics

VOL. E99-C NO. 5
MAY 2016

A PUBLICATION OF THE ELECTRONICS SOCIETY

The Institute of Electronics, Information and Communication Engineers
Kikai-Shinko-Kaikan Bldg., 5-8, Shibakoen 3chome, Minato-ku, TOKYO, 105-0011 JAPAN

BRIEF PAPER

A Clutter Rejection Technique Using a Delay-Line for Wall-Penetrating FMCW Radar

Byungjoon KIM[†a)], Duksoo KIM[†], Youngjoon LIM[†], Dooheon YANG[†], Sangwook NAM[†], *Nonmembers*, *and* Jae-Hoon SONG[†], *Student Member*

SUMMARY This paper proposes a high clutter-rejection technique for wall-penetrating frequency-modulated continuous-wave (FMCW) radar. FMCW radars are widely used, as they moderate the receiver saturation problem in wall-penetrating applications by attenuating short-range clutter such as wall-clutter. However, conventional FMCW radars require a very high-order high-pass filter (HPF) to attenuate short-range clutter. A delay-line (DL) is exploited to overcome this problem. Time-delay shifts beat frequencies formed by reflection waves. This means that a proper time-delay increases the ratio of target-beat frequency to clutter-beat frequency. Consequently, low-order HPF fully attenuates short-range clutter. A third-order HPF rejects more than 20 dB and 30 dB for clutter located at 6 m and 3 m, respectively, with a target located at 9 m detection with a 10,000 GHz/s chirp rate and a 28 ns delay-line.

key words: *clutter rejection, wall-penetrating, FMCW, delay-line, filter*

1. Introduction

Recently, wall-penetrating imaging has been an interesting research topic [1]. An ultra-wideband (UWB) short-pulse radar architecture is one of the candidate radar systems for wall-penetrating imaging [2]. However, this architecture must operate at a high peak power or have a high pulse rate frequency in through-wall applications [3]. To achieve high sensitivity and high dynamic range with a low-power operation, a frequency-modulated continuous-wave (FMCW) radar with a range-gating filter as shown in Fig. 1 (a) can be used to detect targets behind a wall [3], [4].

FMCW radars generate beat frequencies proportional to the differences between their received signals and their chirp signals [5]. Thus, the beat frequency is directly proportional to the stationary target range. Short-range clutter has a lower beat frequency, and long-range clutter has a higher beat frequency. Therefore, an intermediate frequency (IF) or baseband filter attenuates the clutter. The filter consists of a high-pass filter (HPF) to attenuate short-range clutter, and a low-pass filter (LPF) to attenuate long-range clutter and high frequency components (HFC) which are generated during the mixing.

However, a very high-order HPF is required to fully attenuate short-range clutter in conventional FMCW radars. To overcome this problem, the present study exploits the delay-line (DL) as shown in Fig. 1 (b).

Delay-lines have already been used in FMCW radars to linearize voltage-controlled oscillator (VCO) [6], iden-

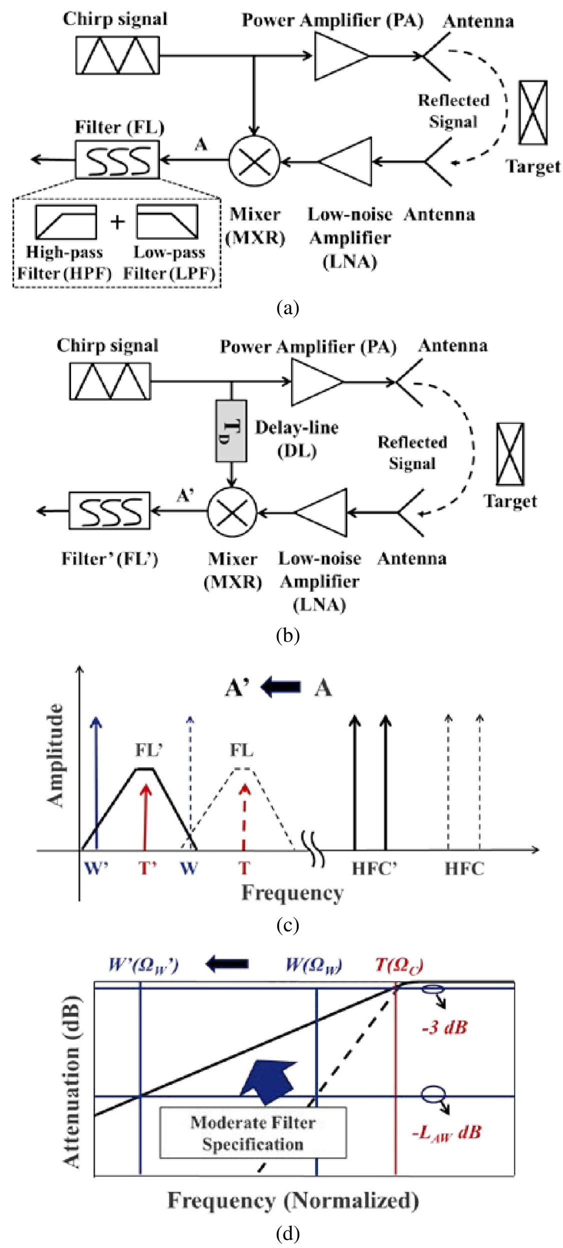

Fig. 1 The architecture of a wall-penetrating FMCW radar; (a) represents a conventional FMCW radar, (b) represents an FMCW radar with a delay-line, (c) represents mixer-output components with a delay-line (solid line) and without a delay-line (dotted line), and (d) represents a normalized high-pass filter specification with a delay-line (solid line) and without a delay-line (dotted line).

Manuscript received November 30, 2015.
[†]The authors are with Seoul National Univ., Seoul, Korea.
a) E-mail: bjkim@ael.snu.ac.kr
DOI: 10.1587/transele.E99.C.597

tify EM sensor cells [7], and obtain wide-altitude ranges [8]. However, in this paper, the delay-line is used to attenuate short-range clutter such as wall-clutter with a low-order HPF.

The inserted delay-line decreases the time gap between the received signal and the chirp signal. Therefore, the beat frequencies of the target and wall are shifted to lower frequencies, and the ratio of pass-band to stop-band frequency is increased. As a result, the low-order HPF meets the filter specification, as shown in Figs. 1 (c) and (d).

In Fig. 1 (c), the dotted line represents the mixer-output components in a conventional FMCW radar, while the solid-line represents the mixer-output components in an FMCW radar with a delay-line. The frequency is shifted constantly by the delay-line so that the wall-beat frequency, W, changes to W' and the target-beat frequency, T, changes to T'. As a result, the ratio of target-beat frequency to wall-beat frequency increases.

The Fig. 1 (d) shows normalized HPF specifications with a delay-line (solid line) and without a delay-line (dotted line). $T(\Omega_C)$ denotes a normalized filter-cutoff frequency, while $W(\Omega_W)$ and $W'(\Omega_W')$ denote a normalized wall frequency without a delay-line and with a delay-line, respectively, and L_{AW} denotes desired attenuation at the wall frequency. As shown in Fig. 1 (d), due to constant frequency shift, the required filter skirt characteristic becomes gradual; this means that a lower order filter can meet the specifications [9].

The following sections explain design methodology, give examples, and present a conclusion. The example is chosen for a short-range target (a stationary target located at 9 m). It is provided for a public service application in which the radar is installed near the wall and target.

2. Design Methodology

FMCW radar systems use a beat frequency to estimate the targets' range [5]. An IF or baseband filter eliminates out-of-range clutter. Therefore, an FMCW radar with an IF filter is highly sensitivity and has a highly dynamic range [3], [4]. Thus, the aforementioned filter is an important component of wall-penetrating FMCW radars.

Such filters consist of LPF and HPF. The LPF attenuates the HFCs generated by the mixer, as well as long-range clutter. The HPF attenuates short-range clutter, such as wall-clutter. In most cases, LPF requirements are low compare with HPF requirements in high-loss wall-penetration applications because the HFCs are far from the target-beat frequency and long-range clutter is weak due to long-range clutter is attenuated dramatically through air propagation and wall-penetration. For example, when a target is located in the middle of a room with the same Radar Cross Section (RCS) wall at 1 m or at 3 m, the nearby wall-clutter amplitude is roughly larger than 79 dB, based on the assumption of a 30 dB one-way wall-penetration attenuation.

The HPF requirements, conversely, are much more difficult to meet. This is because the nearby wall-clutter and other large clutter (i.e., high RCS obstacle) located between the radar sensor and the wall can be much stronger than the target signal [4]. Because target is located at the rear of the wall, its amplitude is largely attenuated through wall-penetration, as a result, its amplitude is relatively small compared with such clutter. The radar sensor requires a much higher-order HPF to fully reject this large clutter.

In the following scenario, assume a conventional low-IF FMCW architecture with a target located at R_T, a wall at R_W, and an obstacle at R_{OC}. The IF is f_0, and the chirp rate is C_R. Then, the beat frequencies are calculated as follows:

$$f_T = f_0 + \frac{2R_T C_R}{c}, \quad f_W = f_0 + \frac{2R_W C_R}{c}, \quad f_{OC} = f_0 + \frac{2R_{OC} C_R}{c} \tag{1}$$

where c is the speed of light, f_T is the target's beat frequency, f_W is the wall's beat frequency, and f_{OC} is the obstacle's beat frequency. Thus, the order of a Butterworth-type HPF can be determined to achieve a desired attenuation [9]:

$$N = \max\left\{ N_W \geq \frac{\log(10^{0.1L_{AW}} - 1)}{2\log\Omega_W},\ N_{OC} \geq \frac{\log(10^{0.1L_{AOC}} - 1)}{2\log\Omega_{OC}} \right\} \tag{2}$$

where N is the filter order, N_W and N_{OC} are the filter order needed to achieve the desired attenuation for wall-clutter and obstacle-clutter, respectively, and L_{AW} and L_{AOC} are the minimum attenuations at Ω_W and Ω_{OC}:

$$\Omega_W = \frac{f_0 c + 2R_T C_R}{f_0 c + 2R_W C_R} \quad \text{and} \quad \Omega_{OC} = \frac{f_0 c + 2R_T C_R}{f_0 c + 2R_{OC} C_R}. \tag{3}$$

For an example, if an obstacle is 3 m, away, the wall is 6 m away, the target 9 m away, the desirable level attenuation of the wall, L_{AW}, is 20 dB, the desirable level attenuation of the obstacle, L_{AOC}, is 30 dB, the IF, f_0, is 10 MHz, and the chirp rate, C_R, is 800 GHz/s, then $N_W \geq 1{,}441.72$ and $N_{OC} \geq 1{,}082.63$. Consequently, a 1,442th-order Butterworth HPF should be chosen. It is not plausible to implement such a high-order filter, so we must increase both Ω_W and Ω_{OC} so the radar effectively rejects clutter with a low-order filter.

Equation (3) shows that high f_0 or low C_R results in low Ω_W and Ω_{OC}, and requires a high-specification HPF. Therefore, a low f_0 or high C_R should be chosen to allow for a low-order HPF. Equation (3) also shows that the maximum achievable values are $\Omega_W = R_T/R_W$, and $\Omega_{OC} = R_T/R_{OC}$ when the conditions meet $f_0 c \ll 2R_W C_R$, and $f_0 c \ll 2R_{OC} C_R$.

Unfortunately, the maximum achievable C_R is limited because chirping-control speed is limited by the device and by circuit technology. The C_R is 857 GHz/s in [3] and the C_R is 2000 GHz/s in [4]. In this example, the filter order dropped to 121 when the C_R is 10,000 GHz/s. Even though the filter order dropped to 121, it is still not plausible to implement such a high-order filter. Therefore, it is preferable to set f_0 to zero or to very low; in particular, zero f_0 not only provides the maximum achievable values of Ω_W and Ω_{OC} but also breaks up the relationship between C_R and filter performance. Thus, the best f_0 is zero from an HPF standpoint for suppressing wall-clutter and obstacle-clutter. If f_0 equals zero, Ω_W equals 1.5 and Ω_{OC} equals 3.0 in the above example. Now a 6th-order Butterworth HPF meets the specifications.

However, a 6th-order filter still entails a high implementation cost. To further moderate the filter requirements, a delay-line can be exploited, as shown in Fig. 1 (b). The delay-line decreases the time gap between a received wave and a chirp signal at mixer and, thus, decreases all beat frequencies uniformly unless the chirp signal enters the mixer LO-port before the received signal enters to the mixer RF-port. If the arrival time of the two signals is reversed, the larger time-delay increases the beat frequency because negative beat frequency folds to become positive. Hence, Eq. (3) should be modified to:

$$\Omega_W = \frac{|2R_T - T_DC|}{|2R_W - T_DC|}, \quad \text{and} \quad \Omega_{OC} = \frac{|2R_T - T_DC|}{|2R_{OC} - T_DC|}, \tag{4}$$

where T_D is the time-delay at the delay-line. Equation (4) implies that a proper time-delay significantly increases Ω_W and Ω_{OC}. Therefore, it is possible to implement a radar system that fully attenuates short-range clutter with a low-order HPF.

The delay-line effect is shown in Fig. 1 (c), which depicts how all the beat frequencies are shifted. In other words, the ratio of the target-beat frequency to clutter-beat frequency is increased. As such increased ratio moderates filter specifications, a low-order filter can also meet the attenuation specifications as shown in Fig. 1 (d).

If there is not a large obstacle between the radar and the wall, then the optimum time-delay is equal to $(2R_W)/c$. The Ω_W increases to infinite, and a simple first-order HPF fully rejects wall-clutter. If a large obstacle exists between the radar and the wall, a graphical method can be used to determine the optimum time-delay.

To minimize the filter order, the optimum time-delay makes N_W equal to N_{OC}. Thus, based on Eq. (2), the following is derived:

$$\Omega_{OC} = {\Omega_W}^A, \tag{5}$$

where $A = \dfrac{\log(10^{0.1L_{AOC}} - 1)}{\log(10^{0.1L_{AW}} - 1)}$.

To find the optimum time-delay for $\Omega_{OC} = {\Omega_W}^A$, a graphical method can be applied directly. The Ω plots versus time-delay, then the $\Omega_{OC} = {\Omega_W}^A$ point is found immediately. The graph in Fig. 2 shows how this works. In the graph, the meeting point between Ω_{OC} (the blue line) and ${\Omega_W}^A$ (the red line) represents the optimum time-delay.

In this example, the optimum time-delay is about 28 ns. If we choose a time-delay as 28 ns, the required HPF order is 3. Note that the filter order, N, should be an integer so that the lowest required filter order is 3.

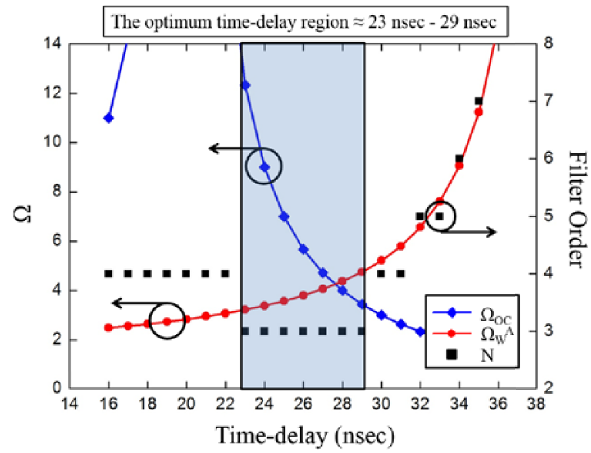

Fig. 2 Ω vs. time-delay graph. Filter order to corresponding is also plotted. (R_T = 9 m, R_W = 6 m, R_{OC} = 3 m, L_{AW} = 20 dB, L_{AOC} = 30 dB, and C_R = 10,000 GHz/s)

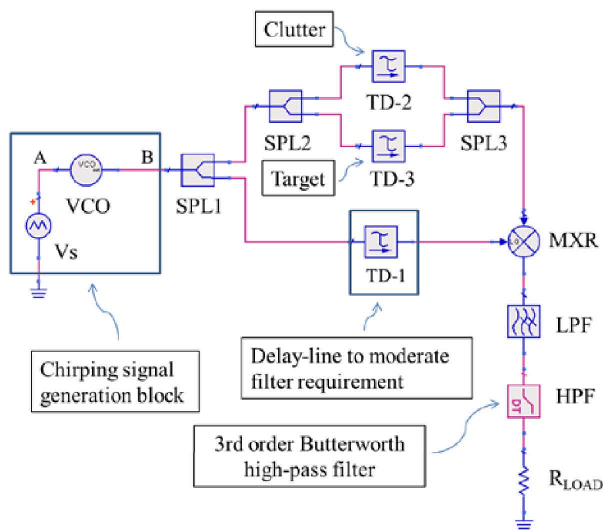

Fig. 3 A simulation setup to verify the proposed system. (R_T = 9 m, R_W = 6 m, R_C = 3 m, L_{AW} = 20 dB, and L_{AC} = 30 dB)

Because the filter order should be an integer, the required filter order remains 3 as long as the time-delay stays within the range of 23 ns to 29 ns. Thus, one is free to choose a time-delay from 23 ns to 29 ns. Notice the required filter order dropped dramatically from 1,442 to 3.

A conventional zero-IF FMCW radar with 10,000 GHz/s chirp rate generates beat frequencies at 200 kHz, 400 kHz, and 600 kHz from the 3 m obstacle, 6 m wall, and 9 m target, respectively. However, the proposed FMCW radar generates beat frequencies at 80 kHz, 120 kHz, and 320 kHz due to the 28 ns time-delay shifting all the beat frequencies. A third-order Butterworth HPF can be designed to attenuate more than 30 dB at 80 kHz, more than 20 dB at 120 kHz, and less than 3.0 dB at 320 kHz.

This has been verified via a system simulation using the Advanced Design System (ADS) [10]. A simulation setup is shown in Fig. 3. An ideal voltage source generates an ideal triangular voltage (0–1 V with 400 us up/down speed,

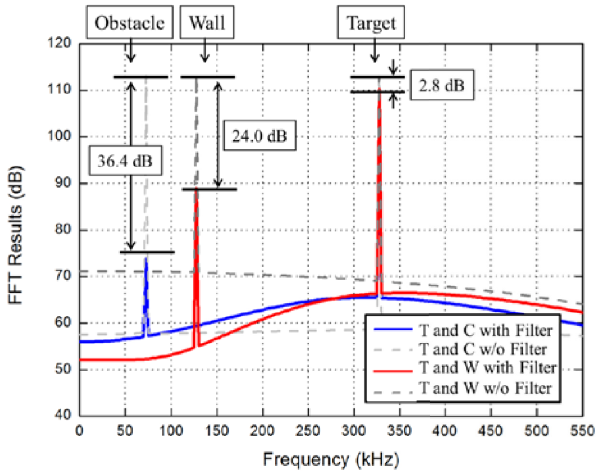

Fig. 4 Simulation results. Target and wall-clutter with and without filter cases and target and obstacle-clutter with and without filter cases are simulated.

at node A). Thus, the ideal VCO generates a chirp signal (100 MHz–4100 MHz, at node B). A splitter (SPL1) splits the signal two ways, sending one signal into the LO-port of the mixer (MXR) and the other into another splitter (SPL2). The SPL2 again splits the signal in two, one signal representing clutter, and the other representing a target. These signal delays corresponding to range. Time-delay components (TD-2, TD-3) are used to represent a target and a wall or an obstacle. TD-3 is set to 60 ns to represent a 9 m target, and TD-2 is set to 40 ns to represent a 6 m wall or is set to 20 ns to represent a 3 m obstacle. The time-delay component (TD-1) represents a delay-line used to moderate filter specifications. It is set to 28 ns, which is the optimum delay for minimizing HPF order. The optimum delay is obtained by using the provided design methodology. The simulation results are shown in Fig. 4. When the same power signals (target and clutter) are injected, the target signal is decreased by 2.8 dB, the wall signal is decreased by 24.0 dB, and the obstacle signal is decreased by 36.4 dB. These results show sound agreement with the theory.

Note that this is assuming the wall and the short-range obstacle locations are already known or have been measured using radar. Also, the technique discussed assumes the target is stationary. Yet, the technique can be applied to a variety of scenarios including moving target scenarios. In fact, as this technique constantly shifts the beat frequencies, the filtered-out signals are only frequency shifted compare with the conventional FMCW radars. Existing processing and algorithms for the conventional FMCW radars (e.g., Doppler processing or Imaging algorithms) can be applied to an FMCW radar with a delay-line simply by compensating for frequency shifting.

3. Conclusion

In this paper, a short-range clutter rejection technique is proposed for wall-penetrating FMCW radar. This method requires only the addition of a simple delay-line at the receiver LO-port to control the time difference between chirp and received signals at the mixer. It allows a low-order HPF to fully attenuate short-range clutter. The validity of this has been verified with a system simulation. This study will help further the implementation of the FMCW radar in wall-penetrating applications.

Acknowledgments

This work was partly supported by the ICT R&D program of MSIP/IITP (No. 14911-01004, SDR Radar Sensor Platform Development).

References

[1] Y. Lim and S. Nam, “Target-to-clutter ratio enhancement of images in through-the-wall radar using a radiation pattern-based delayed-sum algorithm,” Journal of Electromagnetic Engineering and Science, vol.14, no.4, pp.405–410, Dec. 2014.

[2] Y. Yang and A.E. Fathy, “See-through-wall imaging using ultra wideband short-pulse radar system,” Proc. IEEE Antennas Propag. Soc. Int. Symp., pp.334–337, 2005.

[3] G.L. Carvat, L.C. Kempel, E.J. Rothwell, C.M. Coleman, and E.L. Mokole, “A through-dielectric radar imaging system,” IEEE Trans. Antennas Propag., vol.58, no.8, pp.2594–2603, Aug. 2010.

[4] N. Maaref, P. Millot, C. Pichot, and O. Picon, “FMCW ultra-wideband radar for through-the-wall detection of human beings,” Proc. Int. Radar Conference – Surveillance for a Safer World, pp.1–5, Oct. 2009.

[5] B.R. Mahafza, Radar Systems Analysis and Design Using MATLAB, Chapman Hall/CRC, 2000.

[6] L. Reindl, C.C.W. Ruppel, S. Berek, U. Knauer, M. Vossiek, P. Heide, and L. Oreans, “Design, fabrication, and application of precise SAW delay lines used in an FMCW radar system,” IEEE Trans. Microw. Theory Techn., vol.49, no.4, pp.787–794, April 2001.

[7] M.M. Jatlaoui, F. Chebila, S. Bouaziz, P. Pons, and H. Aubert, “Original identification technique of passive EM sensors using loaded transmission delay lines,” Proc. EuMC, pp.1106–1109, Sept. 2010.

[8] J.H. Choi, J.H. Jang, and J.E. Roh, “Optical-delay-based wide-range FMCW radar altimeter,” Elect. Lett., vol.50, no.25, pp.1975–1977, Dec. 2014.

[9] J.S. Hong and M.J. Lancaster, Microstrip Filters for RF/Microwave Applications, Wiley, 2001.

[10] ADS (Advanced Design System: Keysight Technologies) [Online]. Available at: http://www.keysight.com/en/pc-1297113/advanced-design-system-ads?cc=KR&lc=kor/